Wind Turbine Blade Fatigue Tests: Lessons Learned and Application to SHM System Development

S. G. TAYLOR, K. M. FARINHOLT, H. JEONG, J-K JANG,
G. PARK, M. D. TODD, C. R. FARRAR and C. M. AMMERMAN

ABSTRACT

This paper presents experimental results of several structural health monitoring (SHM) methods applied to a 9-meter CX-100 wind turbine blade that underwent fatigue loading. The blade was instrumented with piezoelectric transducers, accelerometers, acoustic emission sensors, and foil strain gauges. It underwent harmonic excitation at its first natural frequency using a hydraulically actuated resonant excitation system. The blade was initially excited at 25% of its design load, and then with steadily increasing loads until it failed. Various data were collected between and during fatigue loading sessions. The data were measured over multiple frequency ranges using a variety of acquisition equipment, including off-the-shelf systems and specially designed hardware developed by the authors. Modal response, diffuse wave-field transfer functions, and ultrasonic guided wave methods were applied to assess the condition of the wind turbine blade. The piezoelectric sensors themselves were also monitored using a sensor diagnostics procedure. This paper summarizes experimental procedures and results, focusing particularly on fatigue crack detection, and concludes with considerations for implementing such damage identification systems, which will be used as a guideline for future SHM system development for operating wind turbine blades.

INTRODUCTION

The authors have been investigating several design parameters of structural health monitoring (SHM) techniques [1] and their performance [2], including ultrasonic guided wave propagation [3] and diffuse ultrasonic wave-field measurements [4], as methods to monitor the health of a wind turbine blade using piezoelectric sensors. The authors have also proposed a multi-scale sensing approach [5, 6] in order to assess the influence of structural damage on the low-frequency dynamic response of a blade. In

Stuart Taylor, Engineering Institute, Los Alamos National Lab., NM, U.S.A.

order to implement these systems in the field, compact sensor nodes, which the authors have been developing [7-9], are necessary. To that end, prototype embedded sensing hardware was tested alongside commercial data acquisition systems. With the proposed sensing strategy, a series of full-scale fatigue tests have been performed in collaboration with Sandia National laboratory (SNL) and the National Renewable Energy Laboratory (NREL). These tests are a precursor for a planned full-scale deployment of an SHM system on 9-meter CX-100 rotor blades to be flown in the field in collaboration with SNL at the U.S. Department of Agriculture's (USDA) Conservation and Production Research Laboratory (CPRL) in Bushland, Texas.

Various methods were implemented using several data acquisition hardware systems. These methods, and oftentimes the hardware systems used, are generally designed for use either with ultrasonic guided waves, typically characterized by a single wave 'packet', often a Gaussian-windowed sinusoid, or with diffuse wave-field measurements, in which a structure is excited with a broadband signal and its response is recorded long past the initial transient response to the excitation. Analysis methods applied include energy methods, cross correlation methods, and time-domain transfer function methods, such as auto-regressive (AR) models or auto-regressive with exogenous inputs (ARX) model-based methods. This paper presents a preliminary analysis of data collected in the course of the fatigue test. The techniques considered are not necessarily optimal detectors, but are a sampling of techniques commonly used in the literature for similar applications.

TEST SETUP

Overview

The test structure employed was a 9-m CX-100 blade [10], originally designed by researchers at SNL. The blade was manufactured according to standard specifications for the CX-100 blade, and it is shown mounted to the test fixture in Figure **1**. The test fixture was a steel frame designed to approximate a fixed-free condition, and oscillatory loads were introduced into the blade using a hydraulically actuated Universal Resonant EXcitation (UREX) system operating at the blade's first resonance.

Figure 1. CX-100 blade mounted on test stand.

The fatigue test was conducted in the fall of 2011. In the fatigue test, the blade was excited intermittently for ~8.5 million cycles until 11/08/11, when a through-thickness fatigue crack surfaced on the leading edge side of the blade's transitional root area. The area including the crack is shown in a photograph in Figure **2**. The surfacing of this crack dramatically altered the dynamic characteristics of the blade, causing the blade's first resonance to vary as a function of loading. However, the authors believe that the damage that ultimately manifested itself as this externally visible crack was detectable using the methods applied in this paper as early as 10/18/11, approximately three weeks prior to the catastrophic failure. In the discussions to follow, the blade will be referred to as 'healthy' for the period prior to 10/20/11, 'damaged' for the period between 10/20/11 and 11/8/11, and 'catastrophically damaged' for the period after 11/8/11.

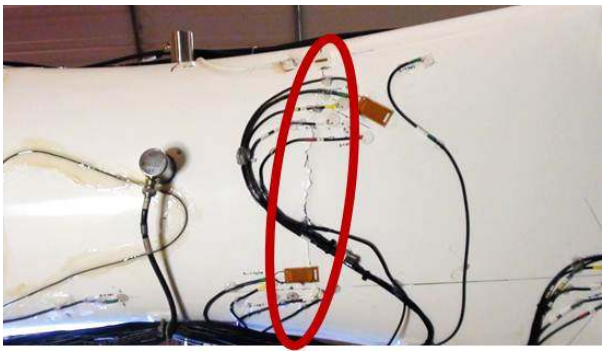

Figure 2. Fatigue crack detail.

Sensor Layout

The low-pressure surface of the blade's root area contained active sensing arrays composed of PZT patches in two configurations: an inner array and an outer array. The sensor arrays on the low-pressure surface of the blade's root area are shown pictorially in the left portion of Figure **3**. The inner array observed a 0.75-m diameter region centered 1 m from the blade root, while the outer array observed a 2-m elliptical region centered 1.5 m from the root.

The high-pressure surface of the blade's root area contained active sensing arrays in only one configuration, corresponding to the inner array on the low-pressure side. The transmission distances ranged from 0.37m to 0.5m, and the actuating patches were located 1 m from the blade root. The sensor arrays on the high-pressure surface of the blade's root area are shown pictorially in the right-hand portion of Figure **3**.

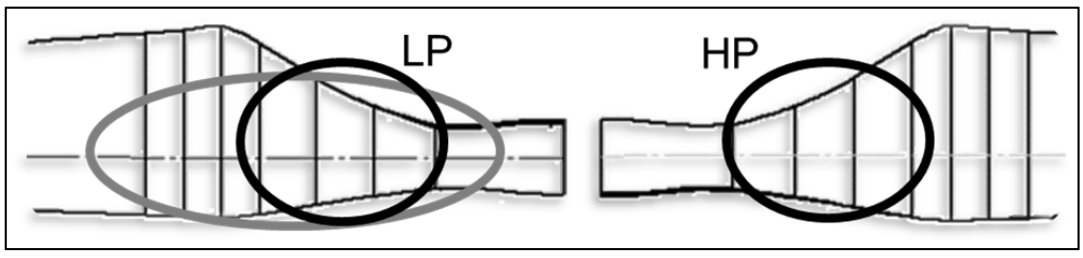

Figure 3. CX-100 root area sensor array locations.

Data Acquisition Systems

The MD7 IntelliConnector [11], by Metis Design, was employed for ultrasonic guided wave analysis over transmission frequencies ranging from 50 kHz to 250 kHz at 25 kHz intervals, with a sampling frequency of 10 MHz. Two IntelliConnectors were deployed to interrogate a 1-m diameter arrays on each side of the blade.

A Bruel & Kjaer LASER data acquisition system was employed for diffuse wave-field measurements, actively interrogating the CX-100 blade with band-limited white nose from 500 Hz to 40 kHz, with a sampling rate of 96 kHz. Its utility in damage detection using diffuse wave field methods had previously been demonstrated using simulated damage in the laboratory [12].

The Wireless Active Sensing Platform (WASP) developed by the authors is a prototype embedded sensor node deployed in order to assess its performance in comparison to commercial systems such as the LASER. Because the WASP's firmware was still in development at the start of the test, it was limited to an effective 20 kHz bandwidth. As with the IntelliConnectors, two WASPs were deployed: one each to interrogate a 1-m diameter array on each side of the blade. For this test, the WASP was configured with a dedicated excitation channel so that an external amplifier could be utilized to ensure a high signal-to-noise ratio.

FATIGUE CRACK DETECTION RESULTS

Ultrasonic Guided Waves

IntelliConnector Data

In this analysis, only the measurements using a 200 kHz excitation signal were considered. For each dataset, the measured response data were match-filtered with the excitation signal in order to reduce the effects of noise, and to discard any response to extraneous inputs. This step would also discard any nonlinear response. A residual was computed by subtracting from each filtered waveform the baseline waveform that resulted in the smallest norm. In computing residuals from the baseline data, only measurements from earlier dates were considered. If the structure remained unchanged, and the training data sufficiently sampled its environmental operating space, the residual would be noise. If the structure had changed, that change would manifest itself as a measureable, deterministic signal.

Because relative phase information is often of little use in guided wave applications, the residual signal was enveloped by computing its instantaneous amplitude via the Hilbert transform. Using this enveloped signal, the normalized residual energy was computed as the ratio of the envelope energy and the energy of the baseline signal used to compute the residual. Dividing the data into 'healthy' and 'damaged' groups based on the dates discussed above, histograms of the normalized residual energy were generated for each sensor path. The histograms were normalized so that they represent discrete probability density functions (PDFs) with total probability of unity. Plots of these histograms are shown in Figure **4**, along with an inset identifying the sensor paths and the location of the fatigue crack, which was between the sensors for paths 3 and 4.

The data for sensor paths 1, 2 and 4 indicate good separability between the underlying states, while paths 3 and 5 indicate moderate separability. Paths 3 and 4 were nearest the crack, and should have been expected to be most affected by it. Path 1 was quite far from the path, but it lay along the blade's carbon fiber spar cap, which may have acted as a wave guide to communicate effects of the underlying damage from the crack location.

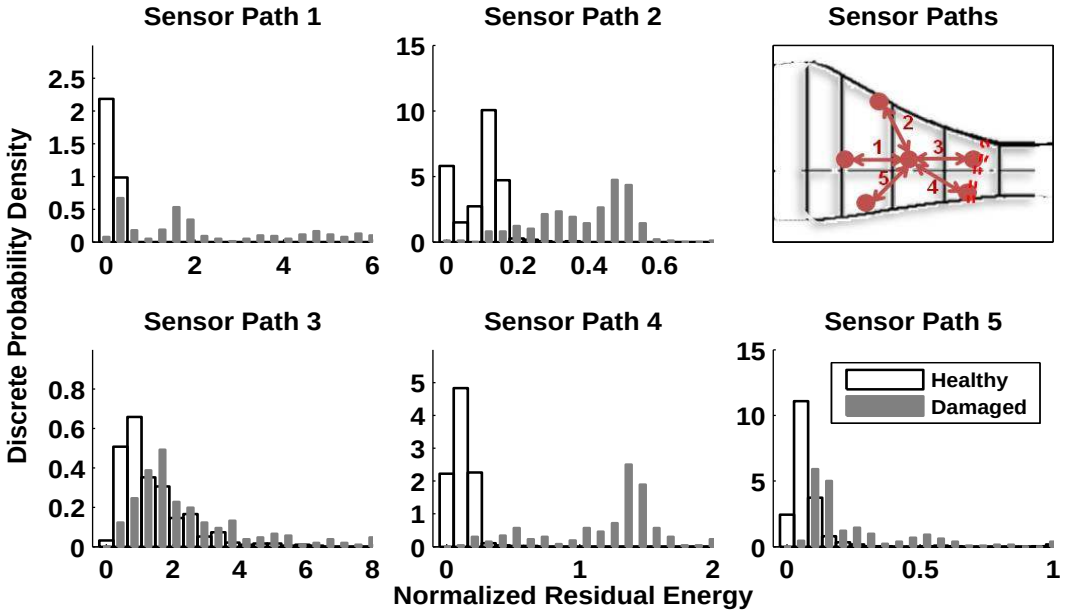

Figure 4. Ultrasonic guided wave normalized residual energy results.

Diffuse Wave Field Transfer Functions

WASP Data

For the analysis of the WASP data, which were obtained using a chirp excitation, an ARX model of order (12, 3) was fit to the data. The exogenous inputs were required because the excitation was not white noise, so the process could not be modeled simply as autoregressive. Treating the model parameters as samples of a multivariate distribution, a covariance matrix was computed, and its eigenvectors were used to compute the principal component loadings for each set of ARX model parameters. In this case, the covariance matrix was computed using only the baseline data, and the principle loads for all data were computed with respect to the baseline.

Sorting the data into 'healthy' and 'damaged' groups based on the test date, histograms of the first principal component were generated, normalizing so that they represent discrete PDFs with unity total probability. Plots of these histograms are shown in Figure **5**, along with an inset identifying the sensor paths and the location of the fatigue crack, which was between the sensors for paths 3 and 4.

There is very little separation in the data for paths 1, 2, and 5, but there is near complete separation in the data for paths 3 and 4, which were physically nearest the crack. This hardware and analysis method combination appears as though it is locally sensitive to structural changes when on or near a sensor path.

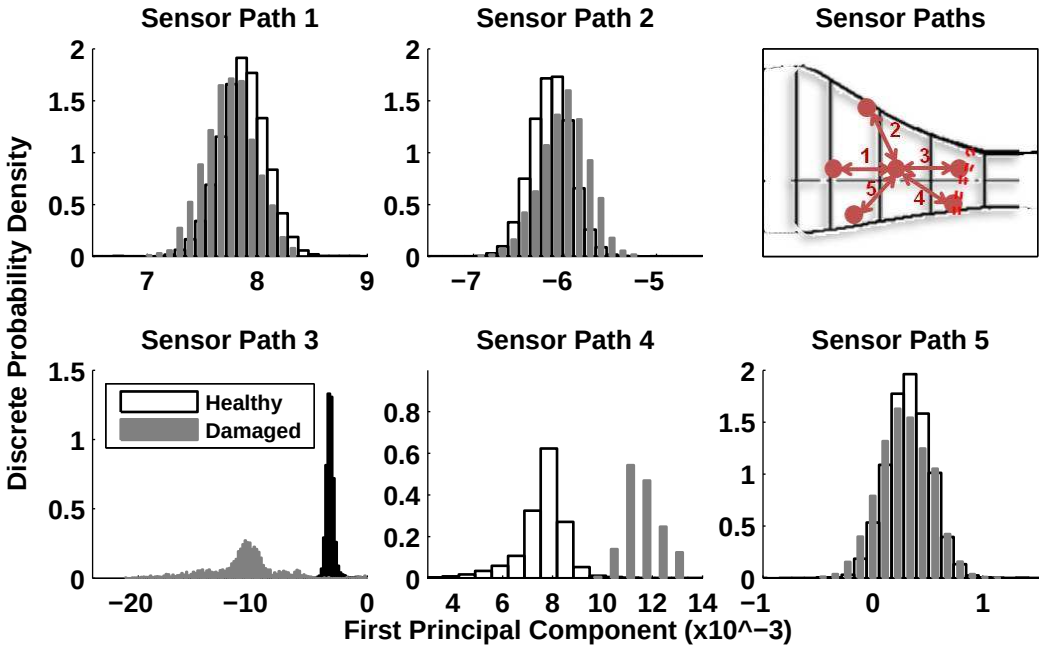

Figure 5. WASP ARX-PCA results.

LASER Data

Using data from the LASER system, cross-correlation (CC) coefficients were computed between newly measured diffuse wave-field frequency response functions (FRFs) and baseline FRFs. A scalar feature was taken as unity minus this CC value. If the newly measured FRF was the same as the baseline, the feature value would be zero, but if the underlying structure changed (e.g. if damage had occurred), the feature value would increase. Dividing the features into 'healthy' and 'damaged' groups based on test date, normalized histograms for each sensor path were generated, and they are plotted in Figure **6**. There is moderate separability between the groups for all sensor paths. This hardware and analysis method combination appears to be generally sensitive to structural change, with somewhat increased sensitivity along the spar cap.

FLIGHT TEST SETUP

Applying lessons learned in the course of the CX-100 blade fatigue test studies, a full-scale CX-100 SHM system deployment is slated for spring 2012, to be conducted in collaboration with SNL at the USDA's CPRL in Bushland, Texas. At the time of this writing, the instrumented blades are being prepared for mounting on the wind turbine tower. While the instrumentation goal for the fatigue test blades was data collection for analysis and learning purposes, the instrumentation on the flight-deployed blade is more targeted and streamlined. The arrays were furthermore installed in the interior of the blade, in order to mitigate the possibility of damage during flight. Two active arrays focus on the blade's trailing edge and leading edge, respectively, one passive array is installed along the blade's carbon-fibre spar cap, which extends down the length of the blade, and one active array mimics those

assessed in this work, on the low-pressure side, inside the root area. While the utility of the first three sensor array types is discussed elsewhere [5, 6], the root area array, will serve to monitor the blade for fatigue damage like that assessed in this work using data from earlier tests. A WASP unit, combined with several analysis methods, including the PCA technique presented above, will be employed for that purpose.

During the fatigue tests, the semi-laboratory environment afforded the luxury of a large impedance analyser; however, such luxury is not practical in the wind turbine hub. For that reason, the prototype WASP hardware has also been designed to perform impedance measurements to assess sensor condition. Sensor diagnostic measurements will be collected prior to each regular structural measurement in order to guarantee that changes in measured responses are indicative of structural changes, rather than sensor failures.

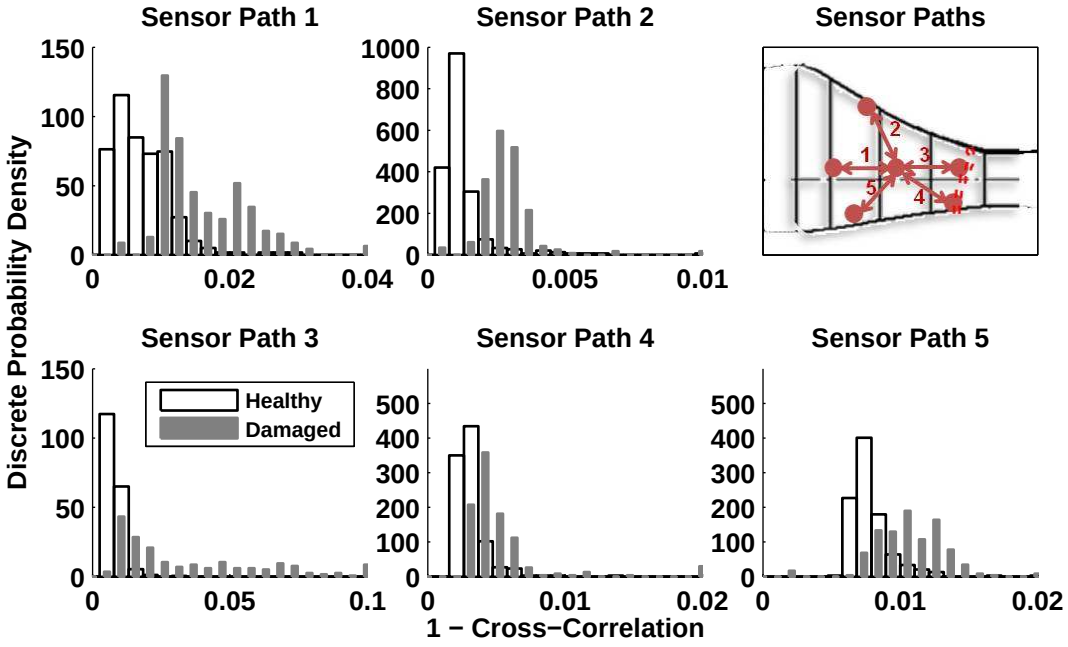

Figure 6. LASER FRF cross-correlation results.

SUMMARY

The fatigue crack detection results of three hardware and analysis method pairs have been presented, all of which indicated reasonable ability to distinguish the 'healthy' from the 'damaged' state of the wind turbine blade. Having demonstrated its ability to detect damage in the blade, the prototype WASP hardware will be deployed on an operational CX-100 wind turbine blade to monitor potential damage formation and collect sensor diagnostic measurements. Four targeted sensor arrays have been installed in a CX-100 blade for this test, including an active array used to monitor the root area of the blade for fatigue damage, and a passive array for correlating the effect of potential fatigue cracks to the global vibration response of the blade.

ACKNOWLEDGEMENTS

This research was funded by the Department of Energy through the Laboratory Directed Research and Development program at Los Alamos National Laboratory, as well as by the Leading Foreign Research Institute Recruitment Program through the National Research Foundation of Korea funded by the Ministry of Education, Science and Technology (2011-0030065). The authors would also like to acknowledge Scott Hughes and Mike Desmond from National Renewable Energy Laboratory, and Mark Rumsey and Jon White from Sandia National Laboratory for their support and guidance on this study.

REFERENCES

[1] C. R. Farrar, and K. Worden, "An introduction to structural health monitoring," Philosophical Transactions of the Royal Society A: Mathematical, Physical and Engineering Sciences, 365(1851), 303-315 (2007).

[2] S. M. Kay, "Fundamentals of statistical signal processing, Volume II: Detection theory," Upper Saddle River (New Jersey), 7, (1998).

[3] S. K. Seth, S. M. Spearing, and S. Constantinos, "Damage detection in composite materials using Lamb wave methods," Smart Materials and Structures, 11(2), 269 (2002).

[4] J. E. Michaels, and T. E. Michaels, "Detection of structural damage from the local temporal coherence of diffuse ultrasonic signals," Ultrasonics, Ferroelectrics and Frequency Control, IEEE Transactions on, 52(10), 1769-1782 (2005).

[5] K. M. Farinholt, S. G. Taylor, G. Park *et al.*, "Full-scale fatigue tests of CX-100 wind turbine blades. Part I: testing." 8343, 83430P-8.

[6] S. G. Taylor, H. Jeong, J. K. Jang *et al.*, "Full-scale fatigue tests of CX-100 wind turbine blades. Part II: analysis." 8343, 83430Q-10.

[7] S. G. Taylor, K. M. Farinholt, E. B. Flynn *et al.*, "A mobile-agent-based wireless sensing network for structural monitoring applications," Measurement Science and Technology(4), 045201 (2009).

[8] S. Taylor, K. Farinholt, G. Park *et al.*, "Multi-scale wireless sensor node for health monitoring of civil infrastructure and mechanical systems," Smart Structures and Systems, 6(5-6), 661-673 (2010).

[9] S. G. Taylor, J. Carroll, K. M. Farinholt *et al.*, "Embedded processing for SHM with integrated software control of a wireless impedance device," SPIE Smart Structures/NDE. 7979, 797904.

[10] D. Berry, [Design of 9-Meter Carbon-Fiberglass Prototype Blades: CX-100 and TX-100] Sandia National Laboratories, Albuquerque, NM(2007).

[11] S. S. Kessler, C. T. Dunn, M. Borgen *et al.*, [A Cable-Free Digital Sensor-Bus for Structural Health Monitoring of Large Area Composite Structures], (2009).

[12] K. Deines, T. Marinone, R. Schultz *et al.*, [Modal Analysis and SHM Investigation of CX-100 Wind Turbine Blade] Springer New York, (2011).